

SOME MODIFICATIONS IN A DYNAMICAL MODEL OF OROGRAPHIC RAINFALL

R. P. SARKER

Institute of Tropical Meteorology, Poona, India

ABSTRACT

A dynamical model presented earlier by the author for the orographic rainfall over the Western Ghats and based on analytical solutions is modified here in three respects with the aid of numerical methods. Like the earlier approximate model, the modified model also assumes a saturated atmosphere with pseudo-adiabatic lapse rate and is based on linearized equations. The rainfall, as computed from the modified model, is in good agreement, both in intensity and in distribution, with the observed rainfall on the windward side of the mountain. Also the modified model suggests that rainfall due to orography may extend out to about 40 km. or so on the lee side from the crest of the mountain and thus explains at least a part of the lee-side rainfall.

1. INTRODUCTION

In a previous paper the author [6] proposed a dynamical model of orographic rainfall with particular reference to the Western Ghats of India and showed that the model explains quite satisfactorily the rainfall distribution from the coast inland along the orography on the windward side. However, the rainfall distribution as computed from that model should be considered only an approximation to the actual orographic rainfall distribution, for, to solve the problem analytically, we were constrained to make the following approximations:

- (i) We took a simplified smoothed profile for the terrain which in reality is not so.
- (ii) We assumed a simplified temperature lapse rate and a steady streamline flow in a neutral atmosphere. The streamline flow may not be fully representative of the real atmosphere which is sometimes to some extent unstable as compared to the pseudoadiabatic lapse rate.
- (iii) We considerably simplified the $f(z)$ profile (viz equation (4), p. 557 of [6]). We divided the atmosphere into three layers (two for the weak monsoon case) in each of which $f(z)$ has a constant but different value.
- (iv) We made a further approximation in the evaluation of the integral in the expression for vertical velocity (viz equation (13), p. 559 of [6]). This approximation is not strictly valid near the crest of the mountain.

The removal of the restrictions (i) to (iv) mentioned above should give us a picture nearer to the actual contribution of orography to rainfall. These restrictions can be removed only by approaching the problem numerically. In this paper we propose to remove the restrictions (iii) and (iv) only. That means we shall give a complete solu-

tion for vertical velocity and streamline displacement from the linearized equations with the real distribution of $f(z)$ as far as possible, subject to the assumption that (a) the ground profile is still a smoothed one, and that (b) the atmosphere is saturated in which both the process and the environment have the pseudo-adiabatic lapse rate.

We shall make another important modification. This is in the lower boundary condition. In this modification, the variation of surface wind $U(\xi_s)$ along the orography caused by the height variation is considered.

Little work has been done on the mountain wave problem by numerical methods. Important contributions in this branch are due to Sawyer [8] and Krishnamurti [2]. Sawyer [8] proposed a quasi-numerical approach to solve the two-dimensional steady-state mountain wave problem with varying $f(z)$ profile for a bell-shaped mountain. In this approach the mean state parameter $f(z)$ is computed from finite difference formulas from prescribed values of wind $U(z)$ and temperature $T(z)$ at 16 levels 1 km. apart. Above 16 km., Sawyer assumed a constant known value for $f(z)$ to great heights. The solution of the vertical wave equation is expressed in terms of definite integrals extending over a wide range of wave numbers. The vertical wave equation is solved by a simple finite difference approach to determine the magnitude of $W(z, k)$ for 32 wave numbers in the range 0 to 5 km.⁻¹ The purpose of this calculation is to obtain the singularities and near singularities in the function $W(z, k)/W(0, k)$ where $W(z, k)$ satisfies equation (1). The solutions for displacement are determined by evaluating the definite integrals including the contribution from the singularities by numerical integration.

Krishnamurti [2] examined the numerical solution of the two-dimensional mountain wave problem in the x - S system of coordinates, where S represents the entropy. In this system the mountain surface itself is treated as a coordinate surface and one can justify a finite-amplitude mountain wave problem by applying the boundary condition along $S=0$. On the other hand, for a finite-amplitude mountain wave, it seems incorrect to apply the boundary condition at $z=0$ in the x - z frame. The mountain profile taken is quite arbitrary. A marching scheme, similar to the scheme used for hyperbolic wave equations in mathematical physics, has been suggested to solve the linear and the non-linear mountain wave problems. It is seen that the marching scheme exactly satisfies the Kelvin monotony condition for uniqueness of the solution.

We shall, however, solve our modified model by a numerical technique similar to the one suggested by Sawyer [8].

2. THE EARLIER MODEL

As pointed out in [6], for a two-dimensional steady laminar flow in the vertical plane xz where the effects of the earth's rotation and of friction are neglected and where the undisturbed quantities are functions of z only and the disturbed quantities are small, the vertical perturbation velocity satisfies the following linearized differential equation:

$$\frac{\partial^2 W(z, k)}{\partial z^2} + [f(z) - k^2]W(z, k) = 0 \tag{1}$$

where

$$f(z) = \frac{g(\gamma^* - \gamma)}{U^2 T} - \frac{1}{U} \frac{d^2 U}{dz^2} + \left(\frac{\gamma^* - \gamma}{T} - \frac{g}{\chi RT} \right) \frac{1}{U} \frac{dU}{dz} - \frac{2}{\chi RT} \left(\frac{dU}{dz} \right)^2 - \left(\frac{g - R\gamma}{2RT} \right)^2 \tag{2}$$

and the vertical perturbation velocity $\omega(x, z)$ is given by

$$\omega(x, z) = \text{Re} \int_0^\infty W(z, k) e^{ikx} \exp\left(\frac{g - R\gamma}{2RT} z\right) dk \cong \text{Re} \left(\frac{\rho_0}{\rho_z} \right)^{1/2} \int_0^\infty W(z, k) e^{ikx} dk. \tag{3}$$

In the above

- U, T, ρ = undisturbed westerly wind, temperature, and density,
- g = acceleration due to gravity,
- γ^* = adiabatic lapse rate, dry or moist,
- γ = actual lapse rate in the undisturbed atmosphere = $-dT/dz$,
- R = gas constant,
- $\chi = g/(g - R\gamma^*)$,
- Re = real part of (),
- z = vertical axis positive upward,
- x = horizontal axis from west to east.

Equation (1) gives the vertical velocity for a sinusoidal ground profile of wave number k from which is obtained the vertical velocity for a smooth arbitrary profile by the method of the Fourier Integral.

We have seen in [6] that for a saturated atmosphere during the southwest monsoon in which both the environment and the process have the pseudo-adiabatic lapse rate, the function $f(z)$ is positive in the lowest layer, it is negative in some middle layer, and again becomes positive above. Accordingly, in [6] we divided the atmosphere into three layers as follows:

$$f(z) \left\{ \begin{array}{l} = l_1^2 \text{ when } z \leq z_0 \\ = -l_2^2 \text{ when } z_0 \leq z \leq H \\ = l_3^2 \text{ when } z \geq H \end{array} \right\}. \tag{4}$$

Under these conditions the solution of equation (1) for the Western Ghats profile

$$\zeta_s(x) = \frac{a^2 b}{a^2 + x^2} + a' \tan^{-1} \left(\frac{x}{a} \right) = \int_0^\infty e^{-ak} \left(ab \cos kx + a' \frac{\sin kx}{k} \right) dk \text{ at } z = -h \tag{5}$$

was of the form

$$\omega_{1,2,3}(x, z) = \text{Re} U(-h) \left(\frac{\rho_s}{\rho_z} \right)^{1/2} \times \frac{\partial}{\partial x} \int_0^\infty e^{-ak} \left(ab - i \frac{a'}{k} \right) e^{ikz} \frac{\Delta_{1,2,3}(z, k)}{\Delta(k)} dk. \tag{6}$$

The expressions $\Delta_{1,2,3}(z, k)$, $\Delta(k)$ are functions of z and k and are given in equation (12), p. 558 of [6]. It was difficult to find an exact value of the integral in equation (6) and an approximate solution was obtained by putting $k=0$ in $\Delta_{1,2,3}(z, k)/\Delta(k)$. When there is no wave this solution becomes

$$\omega_{1,2,3}(x, z) = \text{Re} U(-h) \left(\frac{\rho_s}{\rho_z} \right)^{1/2} \frac{\Delta_{1,2,3}(z, 0)}{\Delta} \times \frac{\partial}{\partial x} \left[ab \frac{a+ix}{a^2+x^2} + a' \left\{ \tan^{-1} \frac{x}{a} + \frac{i}{2} \log_e \frac{a^2+x^2}{a^2} \right\} \right] \tag{7}$$

(see equation (13), p. 559 of [6]). This approximation, as pointed out earlier, is not strictly valid near the crest of the mountain. We call this model for convenience the approximate model.

Our aim in this paper is (i) to take values of $f(z)$ at intervals of 0.25 km. from the surface to 8 km., instead of taking three constant values, and (ii) to find an exact value of the integral corresponding to that in equation (6). For this we approach the problem numerically as follows.

3. THE MODIFIED MODEL

The basic equation (1) has to be solved subject to two boundary conditions. As the lower boundary condition we require that the flow is tangential to the surface. This is given by

$$\frac{d\xi_s}{dx} = \frac{\omega[x, \xi_s(x)]}{U[\xi_s(x)] + u[x, \xi_s(x)]} \quad (8)$$

In view of the restriction to mountains having a shallow slope, a good approximation to the condition (8) is

$$\frac{d\xi_s}{dx} = \frac{\omega(x, 0)}{U[\xi_s(x)]} \quad (9)$$

for a mountain profile at $z=0$. Condition (9) is somewhat inconsistent. We should have taken $\omega[x, \xi_s(x)]$ instead of $\omega(x, 0)$ on the right side of (9). But in that case it would have been extremely difficult, if not impossible, to solve.

If again, the wind shear near the earth's surface is not large, condition (9) can be further approximated to

$$\frac{d\xi_s}{dx} = \frac{\omega(x, 0)}{U(0)} \quad (10)$$

This is called the "linearized lower boundary condition." This condition has been applied by most of the workers in this field. The corresponding linearized boundary condition for our profile (5) is $\omega(x, -h) = U(-h)d\xi_s/dx$ and we have applied this condition in the approximate model of [6].

In his numerical study, Krishnamurti [2] takes the boundary condition

$$\frac{d\xi_s}{dx} = \frac{\omega(x, 0)}{U(0) + u(x, 0)} \quad (11)$$

and so provides for horizontal variation of the surface wind along $z=0$.

In this paper we apply the boundary condition (9) instead of the linearized condition (10) as the wind shear is not small near the earth's surface. We thus account for the variation of surface wind $U[\xi_s(x)]$ along the orography due to its height variation. This condition for our profile (5) is

$$\omega(x, -h) = U(\xi_s) \frac{d\xi_s(x)}{dx} \quad (12)$$

This gives

$$W(-h, k) = \left(\frac{\rho-h}{\rho_0}\right)^{1/2} U(\xi_s) e^{-ak} \left(ab - i \frac{a'}{k}\right) ik \quad (13)$$

The upper boundary condition poses a problem. The solution of equation (1) is strictly indeterminate unless the values of $f(z)$ are specified to indefinitely great heights. However, it is physically unlikely that the computed flow pattern in the lower troposphere will be greatly affected by the wind and temperature in the upper troposphere and stratosphere. We have seen in [6] that during the monsoon, $f(z)$ above 8 km. or so becomes indeterminate because of

the change of direction of wind from westerly to easterly. We, therefore, assume for numerical integration of equation (1) that above a level of 8 km. the atmosphere is such that $f(z)$ is constant and equal to a specified value L . The choice of L has only very small effect at low levels (Palm and Foldvik [4], Corby and Sawyer [1], and Sawyer [8]). For simplicity we assume that $L=0.0 \text{ km.}^{-2}$ This is tantamount to assuming that the wind speed and direction above 8 km. remain constant for the saturated atmosphere that we are considering.

The approximate solution of equation (1) in the region above 8 km. where $f(z)$ is constant and equal to 0.0 is of the form

$$W(z, k) = A \exp(-kz) \quad (14)$$

Since the pressure and vertical velocity are continuous, we require that $W(z, k)$ and $\partial W/\partial z$ are continuous functions of z . Equation (14) can therefore be used to provide the boundary condition at the level $z=z_1=8 \text{ km.}$ which is used as the upper limit for numerical solution of equation (1). This is

$$\frac{\partial}{\partial z} W(z, k) = -kW(z, k) \text{ at } z=z_1 \quad (15)$$

To solve equation (1) numerically we specify a function $\psi(z, k)$ satisfying equation (1) and satisfying equation (15) at $z=z_1=8 \text{ km.}$ Thus

$$\frac{\partial^2 \psi(z, k)}{\partial z^2} + [f(z) - k^2]\psi(z, k) = 0 \quad (16)$$

and

$$\frac{\partial \psi(z, k)}{\partial z} = -k\psi(z, k) \text{ at } z=z_1 \quad (17)$$

We also assume for convenience

$$\psi(z_1, k) = 1 \quad (18)$$

Then $W(z, k)$ is a simple multiple of $\psi(z, k)$ which satisfies the lower boundary condition (13). Thus

$$W(z, k) = \left(\frac{\rho-h}{\rho_0}\right)^{1/2} U(\xi_s) \left(ab - i \frac{a'}{k}\right) ik \cdot \frac{\psi(z, k)}{\psi(-h, k)} e^{-ak} \quad (19)$$

The vertical velocity, according to equation (3) is thus given by

$$\omega(x, z) = \text{Re} \left(\frac{\rho-h}{\rho_0}\right)^{1/2} U(\xi_s) \int_0^\infty \left(ab - i \frac{a'}{k}\right) ik \cdot \frac{\psi(z, k)}{\psi(-h, k)} e^{-ak} \cdot e^{ikz} dk \quad (20)$$

With the values of $\psi(z, k)$ obtained according to equations (16), (17), and (18), the integration in (20) is performed numerically to get the vertical perturbation velocity caused by the mountain. However, difficulty arises in numerical integration if the function $\psi(-h, k)$ vanishes for some values of k in the range of integration.

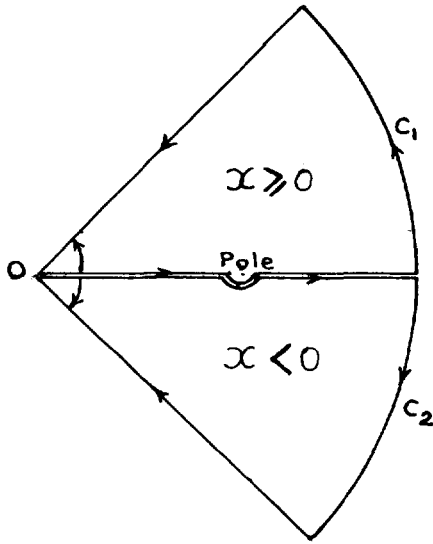


FIGURE 1.—Paths of contour integration of equation (22).

For that value of k the integrand has singularity and it is this singularity that gives rise to lee waves. The numerical integration of equation (20) is made possible by first subtracting from the integrand a function which has similar behavior near the singular point. Such a function is

$$\frac{\psi(z, k_r) \exp(-ak + ikx)}{\psi'(-h, k_r)(k - k_r)} \left(ab - i \frac{a'}{k}\right) ik \quad (21)$$

where $k = k_r$ is a singular point and

$$\psi'(-h, k_r) = \left[\frac{\partial}{\partial k} \psi(-h, k) \right]_{k=k_r}$$

The expression (21) has a simple pole at $k = k_r$ with the same residue as the integrand in (20). We thus write equation (20) in the form

$$\begin{aligned} \omega(x, z) = & \operatorname{Re} \left(\frac{\rho - h}{\rho_z} \right)^{1/2} U(\zeta_s) \left\{ \int_0^\infty \left[\frac{\psi(z, k)}{\psi(-h, k)} \right. \right. \\ & \left. \left. - \sum_r \frac{\psi(z, k_r)}{\psi'(-h, k_r)(k - k_r)} \right] \times \left(ab - i \frac{a'}{k}\right) ik \right. \\ & \left. \times \exp(-ak + ikx) dk + \sum_r \frac{\psi(z, k_r)}{\psi'(-h, k_r)} \int_0^\infty \left(ab - i \frac{a'}{k}\right) ik \right. \\ & \left. \times \frac{\exp(-ak + ikx)}{k - k_r} dk \right\} \quad (22) \end{aligned}$$

where the summation extends over all the singularities in the range of integration. The integrand in the first integral of (22) is now free from singularities and numerical integration can be carried out. The second integral is the lee-wave term and is best evaluated by contour integration. We choose the path of contour integration as shown in figure 1 so as to place the lee wave on the downstream side. Performing the integration and making

the radius of indentations tend to zero and the radius of the circular arc tend to infinity we find

$$\begin{aligned} & \int_0^\infty \left(ab - i \frac{a'}{k}\right) ik \cdot \frac{\exp(-ak + ikx)}{k - k_r} dk \\ & = i(1+i)^2 \int_0^\infty k \left\{ ab - \frac{a' i(1-i)}{2k} \right\} \\ & \quad \times \frac{\exp\{[-(a+x) + i(x-a)]k\}}{k(1+i) - k_r} dk \\ & \quad + 2\pi i \cdot ik_r \left(ab - i \frac{a'}{k_r}\right) \exp(-ak_r + ik_r x) \text{ for } x \geq 0 \\ & = i(1-i)^2 \int_0^\infty k \left\{ ab - \frac{a' i(1+i)}{2k} \right\} \\ & \quad \times \frac{\exp\{[-(a-x) + i(x+a)]k\}}{k(1-i) - k_r} dk \text{ for } x < 0. \quad (23) \end{aligned}$$

It is seen that a term of the form $2\pi i \exp(-ak_r + ik_r x)$ appears for $x \geq 0$. This is the lee-wave term. With our choice of boundary condition above 8 km., k_r happens to be real, so that the lee-wave term represents a simple harmonic wave train extending indefinitely downstream.

From (22) and (23) the complete solution for the vertical velocity can be written as

$$\omega(x, z) = \left(\frac{\rho - h}{\rho_z}\right)^{1/2} U(\zeta_s) \{ \operatorname{Re}(x_1 + x_2 + x_3) \} \quad (24)$$

where

$$x_1 = \int_0^\infty \left(\frac{\psi(z, k)}{\psi(-h, k)} - \sum_r \frac{\psi(z, k_r)}{\psi'(-h, k_r)(k - k_r)} \right) \left(ab - i \frac{a'}{k}\right) ik \times \exp(-ak + ikx) dk \quad (24a)$$

$$\begin{aligned} x_2 = & \sum_r \frac{\psi(z, k_r)}{\psi'(-h, k_r)} i(1+i)^2 \int_0^\infty k \left\{ ab - \frac{a' i(1-i)}{2k} \right\} \\ & \times \frac{\exp\{[-(a+x) + i(x-a)]k\}}{k(1+i) - k_r} dk \quad \left. \vphantom{\sum_r} \right\} \text{ for } x \geq 0 \\ x_3 = & 2\pi i \sum_r \frac{\psi(z, k_r)}{\psi'(-h, k_r)} ik_r \left(ab - i \frac{a'}{k_r}\right) \\ & \times \exp(-ak_r + ik_r x) \quad (24b) \end{aligned}$$

$$\begin{aligned} x_2 = & \sum_r \frac{\psi(z, k_r)}{\psi'(-h, k_r)} i(1-i)^2 \int_0^\infty k \left\{ ab - \frac{a' i(1+i)}{2k} \right\} \\ & \times \frac{\exp\{[-(a-x) + i(x+a)]k\}}{k(1-i) - k_r} dk \quad \left. \vphantom{\sum_r} \right\} \text{ for } x < 0 \\ x_3 = & 0. \quad (24c) \end{aligned}$$

4. METHODS OF NUMERICAL EVALUATION

To evaluate the expressions in equation (24) a program was written for the electronic computer CDC 3600 of Tata Institute of Fundamental Research, Bombay, for an airstream with specified arbitrary values of $f(z)$ at 0.25-km.

intervals of height from 0 to 8 km. For the purpose of numerical integration of (1) a height interval of 0.25 km. was chosen.

EVALUATION OF ψ AND ψ'

Numerical integration of equation (1) is carried out for 32 values of k in the range 0 to 5 km.⁻¹. Intervals used for k are 0.05 km.⁻¹ from 0 to 1 km.⁻¹, 0.2 km.⁻¹ from 1 to 2 km.⁻¹, and 0.5 km.⁻¹ for $k > 2$ km.⁻¹. Equation (16) is written in the simple finite difference form

$$\psi_{r-1} = -\psi_{r+1} + [2 - d^2(f_r - k^2)]\psi_r \tag{25}$$

where d is the finite difference interval of 0.25 km.

Integration is started at the 32d interval corresponding to 8 km. at which

$$\psi_{32} = 1. \tag{26}$$

Condition (17) was used in the finite-difference form to give the second condition

$$\psi_{31} = 1 + \frac{k^2 d^2}{2} + kd. \tag{27}$$

Values of $\psi'(-h, k)$ were obtained by solving a similar finite-difference equation obtained by differentiating (25) with respect to k subject to the boundary conditions obtained by differentiating (26) and (27). Thus

$$\psi'_{r-1} = -\psi'_{r+1} + [2 - d^2(f_r - k^2)]\psi'_r + 2kd^2\psi_r \tag{28}$$

is solved subject to

$$\psi'_{32} = 0 \tag{29}$$

and

$$\psi'_{31} = kd^2 + d. \tag{30}$$

With these expressions the values of ψ and ψ' are obtained for 33 levels of height from 0 to 8 km. and for 32 values of k from 0 to 5 km.⁻¹

LOCATION OF SINGULARITIES OF $\psi(x, k)/\psi(-h, k)$

It appears from the boundary condition at $z = z_1$ that all the values of ψ and ψ' are real. A preliminary zero of $\psi(-h, k)$ was located from the alternating signs of $\psi(-h, k)$ calculated for the 32 values of k . This preliminary zero was used as a starting point for an iterative Newton-Raphson method which locates the zero of $g = \psi(-h, k)$. This is based upon the recurrence relation

$$k_{s+1} = k_s - g_{k=k_s} / \left(\frac{\partial g}{\partial k} \right)_{k=k_s} \tag{31}$$

EVALUATION OF THE INTEGRALS IN EQUATIONS (24a)-(24c)

The integrand in the expression (24a) can be expressed in a form $A(k) \exp(ikx)$; that in expression (24b) in a form $A(k) \exp\{ik(x-a)\}$; and that in expression (24c) in a form $A(k) \exp\{ik(x+a)\}$ where the function $A(k)$ is seen to vary

slowly with k . On the other hand, the factors $\exp(ikx)$, $\exp\{ik(x-a)\}$, and $\exp\{ik(x+a)\}$ oscillate rapidly with k for large values of $|x|$. We use the following formula for integration between two successive ordinates $k = k_1$ and $k = k_2$:

$$\int_{k_1}^{k_2} A(k) \exp(ikx) dk = \frac{2}{x} \left\{ \sin \frac{k_2 - k_1}{2} x \right\} \times \frac{A_1 + A_2}{2} \exp\{ix(k_1 + k_2)/2\} - \frac{i}{x} \left\{ \cos \frac{k_2 - k_1}{2} x - \frac{2}{x(k_2 - k_1)} \sin \frac{k_2 - k_1}{2} x \right\} \times (A_2 - A_1) \exp\{ix(k_1 + k_2)/2\}. \tag{32}$$

The above formula has been obtained on the assumption that $A(k)$ varies very slowly with k so that its derivative is constant in the range k_1 to k_2 . This relation has been used to evaluate the contribution of the interval between pairs of successive values of k to the integrals in (24a), (24b), and (24c). The intervals used in the integration are 0.05 km.⁻¹ from 0 to 1 km.⁻¹, 0.2 km.⁻¹ from 1 to 2 km.⁻¹, and 0.5 km.⁻¹ for $k > 2$ km.⁻¹

ERRORS IN THE NUMERICAL SOLUTION

To find the values of ψ and ψ' , equation (16) was put into the finite difference form (25). Truncation error is to be expected in the use of the finite-difference equations (25) and (28). In ignoring the 4th-order difference and substituting

$$\frac{\partial^2 \psi}{\partial z^2} = (\psi_{r+1} + \psi_{r-1} - 2\psi_r) / d^2$$

a proportionate error of the order of $f(z)d^2/12$ is made. Typical values of $f(z)$ under study are less than 1 km.⁻², the maximum values never exceeding 2.0 km.⁻² Thus with $d = 0.25$ km. the error is less than 1 percent although it may rise to 1 percent occasionally. With these considerations in mind it is believed that the computed values of $\omega(x, z)$ represent the true solution of equation (20) within a few percent.

From the vertical velocities computed, the displacements $\zeta(x, z)$ of the streamlines above their original undisturbed level z were computed from the formula:

$$\omega(x, z) = U(z) \frac{\partial \zeta(x, z)}{\partial x} \tag{33}$$

by using a marching scheme. The solution $\zeta(x, z)$ for $z = -h$ was used to reconstruct the mountain profile. Comparison of this solution with the actual profile given by equation (5) showed that the error was less than 5 percent everywhere and there appears no reason to expect greater errors in the evaluation of $\zeta(x, z)$ at other levels.

THE PROGRAM ON CDC 3600

The program as written for the computer CDC 3600 provides for the specification of $f(z)$ at 0.25-km. intervals

TABLE 1.—Computed wavelengths of the different cases

Case no.	Date	Wavelength in km.
I.....	July 5, 1961.....	19.2
II.....	June 25, 1961.....	29.2
III.....	July 6-9, 1963.....	29.6
IV.....	July 11-12, 1965.....	31.7
V.....	July 21, 1959.....	26.5

from 0 to z_1 km. and for the specification of z_1 , the upper limit of numerical integration, and the mountain parameters a , b , a' . Also specification was provided for $U(-h)(\rho_{-h}/\rho_2)^{1/2}$ at 1-km. intervals. Values of $\omega(x, z)$ were calculated at horizontal interval of 2 km. extending for 50 intervals on either side of the origin. Also a program was made for computing $\zeta(x, z)$, the displacements of the streamlines from the vertical velocities. To compute these values of $\omega(x, z)$ and $\zeta(x, z)$ for eight levels takes about 4 min. on the CDC 3600. It should be mentioned here that we computed vertical velocity first for the linearized lower boundary condition, viz, replacing $U(\zeta_s)$ by $U(-h)$ in equation (24), and then we accounted for the modified boundary condition (12) by multiplying the computed vertical velocity by $U(\zeta_s)/U(-h)$.

5. RESULTS

Using the above method, we have computed vertical velocity set up by the mountain. Corresponding to the vertical velocity so obtained we have computed rainfall intensity and its distribution along the orography, taking into consideration the downwind extension of precipitation elements as in [6]. We have taken cases 1-5 of [6] so that we can compare the orographic rainfall distribution computed from the present modified model with that obtained from the approximate model presented in [6].

Before we discuss the results of rainfall distribution, it is worthwhile here to mention the following interesting results obtained from the model. We have seen that in none of the seven cases presented in the approximate three-layer model in [6], did lee waves occur. But the results are different when we examine these cases in detail in this model. It is seen that $\psi(-h, k)$ invariably vanishes in each case for some real value of k . Also we have seen it vanishes only once indicating the existence of only one sinusoidal wave for each case. The wavelengths for the five cases are given in table 1. They vary in the range 19-32 km. We thus see that it is possible to have lee waves excited by a mountain in a statically neutral atmosphere, if the wind shear is favorably distributed. It may be mentioned here that all the earlier workers in this field have stressed the need of both stability and wind shear for occurrence of lee waves and have thought that stability is a prerequisite condition for existence of lee waves. The present result leads us to infer that while stability is an important factor for the occurrence of mountain waves, as examined by the author [7] earlier, it is by no means a necessary condition. Even in a statically neutral layer, it is quite possible for stationary lee waves

to exist as a result of wind shear. The situation, however, might be different in a time-dependent solution.

Incidentally, we note that we have seen in our study of mountain waves [7] that mountain waves of length 60-70 km. can occur on the lee of the Western Ghats during the winter months, and also three or four waves may superpose on one another in that season. But during the monsoon the waves are of length 20-30 km. only and not more than one wave appears to exist then. While the larger waves of the winter season may have some importance to aviation, the shorter waves of the monsoon may contribute to rainfall on the lee side.

We now discuss the rainfall distribution for the five cases.

CASE I—JULY 5, 1961

The vertical velocity distribution with height z and horizontal distance x as computed from the present model is given in figure 2 a, b, c. Comparison of these with figure 6 a, b of [6] reveals the following common features of vertical velocity computed from the two models. The vertical velocity in both the models increases along the mountain from the coast toward the crest. This continues to $x = -10$ km., i.e., 15 km. before the crest. The magnitude then decreases. Also, the vertical velocity first increases with height, then decreases and gradually becomes negative. However, there are some differences between the vertical velocities computed from the two models. To start with, the velocity near the coast is less in the present model than in the approximate model of [6]. This is true as far as $x = -40$ km. Beyond this, the vertical velocity is greater in the present model. For example, the maximum vertical velocity is 70 cm. sec.⁻¹ at $x = -10$ km. in the present model, whereas the corresponding value in the approximate model is 33 cm. sec.⁻¹. On the windward side, vertical velocity may be positive up to the height of 8 km. in the approximate model. But in the present model the velocity is negative above 5 km. Also in the approximate model, velocity is negative at all levels beyond $x = 3$ km. But in the present model beyond $x = 3$ km. velocity is negative generally up to the height of 4 km., above which the velocity is positive. This is due to the lee wave of length 19 km. This continues to about $x = 20$ km. after which it is negative at all levels. Subsequently the values become positive and negative alternately.

The rainfall distribution along the orography is given in figure 3. The solid line shows the observed intensity and the dashed line the orographic intensity as computed in [6]. The dashed-dotted line represents the orographic intensity as computed from the present modified model.

The orographic rainfall at the coast is 1.2 mm./hr. as computed from the approximate model and only 0.5 mm./hr. as computed from the present model. The orographic rainfall computed from the present model falls short of the intensity computed from the approximate model up to $x = -30$ km., after which rainfall computed from the present model is more than that computed from the approximate model. The highest observed rainfall is

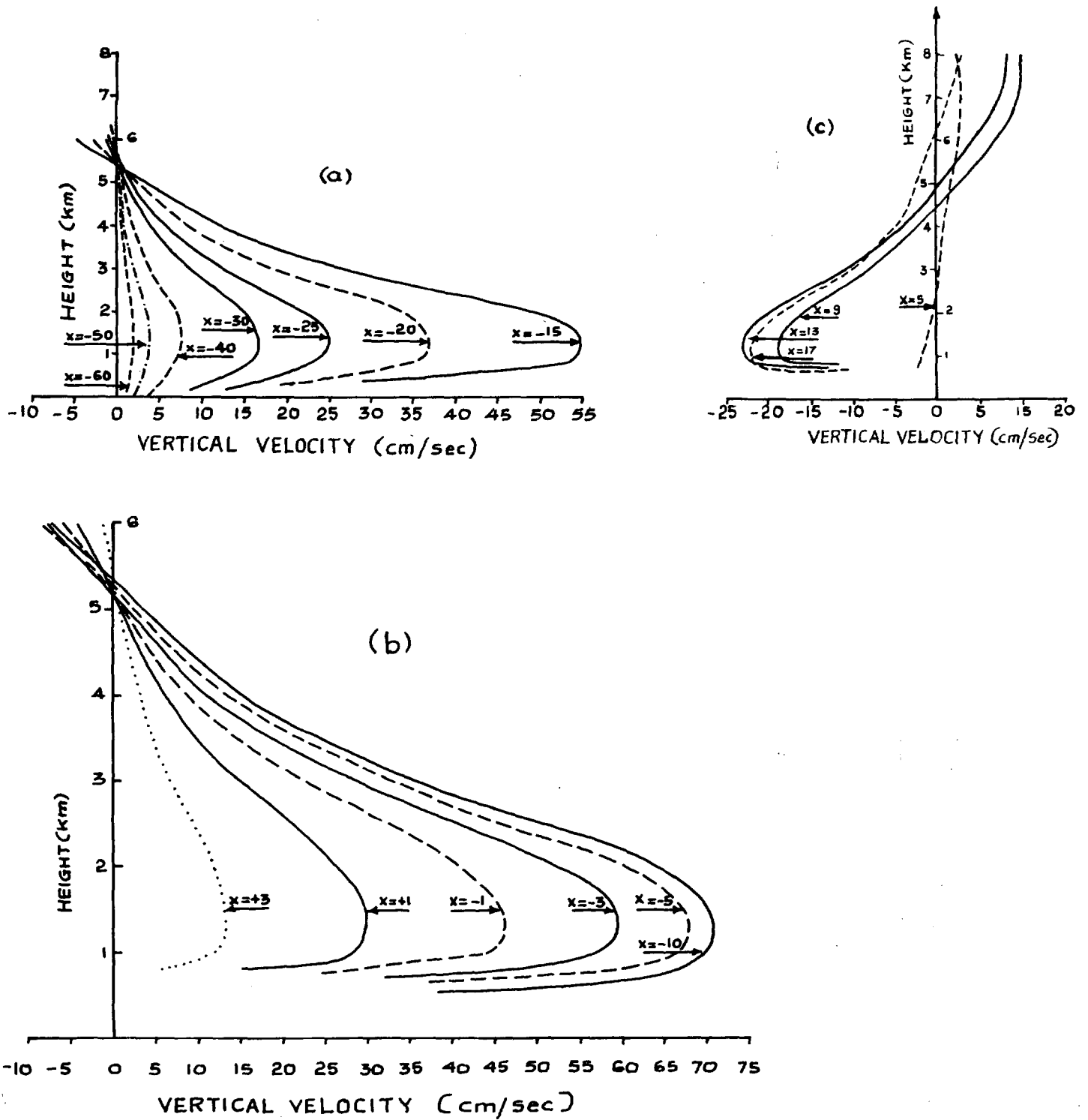


FIGURE 2.—Perturbation vertical velocity W (cm./sec.) profiles at different distances x along the orography on July 5, 1961 (Case I) as computed from the present modified model. $x=5$ is the crest of the mountain and $x=-60$ is the coastal position. (a) Profile for -60 km. $\leq x \leq -15$ km. (b) Profiles for -10 km. $\leq x \leq 3$ km. (c) Profiles for 5 km. $\leq x \leq 17$ km.

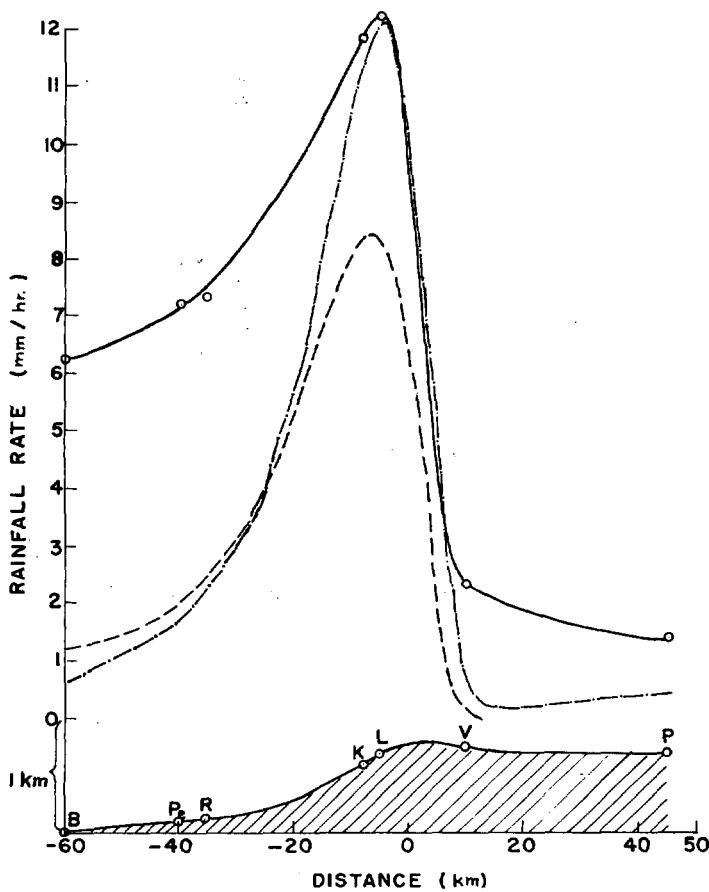


FIGURE 3.—Observed (upper solid curve), computed orographic from the approximate model of [6] (dashed curve), and computed orographic from the present modified model (dashed-dotted curve) rainfall distribution for July 5, 1961 (Case I) along the orographic profile (shaded) from the coast at Bombay (B) inland through Pen (Pe), Roha (R), Khandala (K), Lonavla (L), Vadgaon (V), and Poona (P).

12.2 mm./hr. and the highest orographic rainfall is 12.0 mm./hr. computed from the present model; that from the approximate model is 8.4 mm./hr. only. Thus the maximum orographic rainfall computed from the present model is 98 percent and that from the approximate model is 69 percent of the observed maximum rainfall. Also there is very good agreement between the positions of the peaks of observed and computed rainfalls. The rainfall values, observed as well as computed, drop sharply beyond the peak values. There is very close agreement between the observed rainfall and the rainfall computed from the present model up to $x=5$ km., i.e., the crest of the mountain. The observed rainfall, and that computed from the present model are both 4 mm./hr. at the crest of the mountain. But the corresponding value from the approximate model is 2 mm./hr. The orographic rainfall computed from the present model is very small beyond $x=5$ km. It goes down to 0.2 mm./hr. at $x=16$ km. and then again gradually rises to 0.4 mm./hr. at $x=40$ km. The computed rainfall on the lee side, however, is very small compared to observed rainfall.

It appears that computed orographic rainfall in the windward side originates from levels at and below 5 km., whereas the lee-side rainfall has generating cells at 6 km. and above.

It should be mentioned here that while computing rainfall for ascending motion at high levels on the lee side, we have made the necessary modifications for unsaturated conditions of an air parcel which, initially saturated, becomes unsaturated in the course of its descending motion and then again starts to ascend.

CASE II—JUNE 25, 1961

The vertical velocity distribution with height z and horizontal distance x , as computed from the present model and from the approximate model, exhibit features similar to those in Case I. For example, the vertical velocity on the windward side, as computed from the approximate model, may be positive up to 7.5 km. (the limit of our study in this case), but in the present model the velocity is negative above 5 km. The maximum vertical velocity in this case is 29 cm. sec.⁻¹ at $x=-10$ km. for the approximate model and that for the present model is 36 cm. sec.⁻¹ In the approximate model, the velocity is negative at all levels beyond $x=2$ km. But in the present model beyond $x=2$ km. velocity is positive at 3 km. and above. This continues up to $x=20$ km.

The rainfall distribution along the orography is given in figure 4. Although the orographic rainfall distributions computed from the present model and the approximate model, follow the same pattern of distribution as the observed rainfall from the coast to the crest of the mountain, there is some difference between the orographic intensities computed from the two models. Compared to the observed rainfall of 2 mm./hr. at the coast, the computed orographic rainfall is 1.2 mm./hr. from the approximate model and is only 0.4 mm./hr. from the present model. To about $x=-20$ km. the approximate model appears to overestimate the contribution of orography. The maximum orographic rainfall computed from the approximate model is 90 percent of the observed maximum value. But that computed from the present model is 98 percent. There is close agreement between the positions of the maximum observed and computed values. They differ by about 2 km. At the crest of the mountain, rainfall, observed as well as computed from the two models, is 3 mm./hr. Orographic rainfall computed from the approximate model is nil beyond 10 km. from the crest of the mountain. But the computed value from the present model extends beyond 40 km. from the crest of the mountain. Also in the rainfall computed from the present model, there is a secondary maximum of 1.7 mm./hr. at $x=30$ km. i.e., at 25 km. beyond the crest. At Poona ($x=45$ km.) the computed rainfall agrees with the observed rainfall. The secondary maximum on the lee side could not be verified, as in the area considered we do not have any rain-reporting stations between Vadgaon and Poona.

As mentioned in Case I, the computed rainfall on the windward side has its origin confined below 5 km., but

that on the lee side has its origin at and above 5 km. This appears to be substantiated by radar observations (Pisharoty [5], Mani et al. [3]).

CASE III—JULY 6-9, 1963

As before, the vertical velocity on the windward side may be positive up to 7 km. (maximum limit of integration in this case) in the approximate model, but it is negative above 4.0 km. in the present model. Near the coast the vertical velocity is more in the approximate model. For example, at $x = -50$ km., maximum vertical velocity is $5.5 \text{ cm. sec.}^{-1}$ in the approximate model, but in the present model the corresponding value is $2.8 \text{ cm. sec.}^{-1}$. Beyond $x = -30$ km. the vertical velocity given by the present model is more. The vertical velocity is maximum for $x = -10$ km., the corresponding values being 24 cm. sec.^{-1} and 50 cm. sec.^{-1} in the approximate model and the present model respectively. In the approximate model, vertical velocity is negative at all levels beyond $x = 0$ km. But in the present model velocity is positive at low levels to $x = 3$ km., after which velocity is negative at low levels and positive at levels above 3 km. due to the wave of length 20 km. This continues to $x = 17$ km.

The rainfall distributions, observed as well as computed from the two models, are given in figure 5. As in the previous cases, the approximate model overestimates the rainfall due to orography to about $x = -20$ km. At the coast the orographic rainfall computed from the approximate model and the present model are 1.4 mm./hr. and 0.3 mm./hr. , respectively, compared to the observed intensity of 2.4 mm./hr. The maximum orographic rainfall intensities computed from the approximate model and the present model are 5.9 mm./hr. and 7.3 mm./hr. , respectively, compared to observed maximum of 7.8 mm./hr. That is, the orographic maximum computed from the two models is respectively 76 percent and 94 percent of the observed maximum. Also the agreement between the position of the orographic rainfall maximum computed from the present model with the position of the observed maximum is very good. They differ at most by 1 km. But the position of the orographic maximum computed from the approximate model differs by about 4-5 km. from the position of the observed maximum. Beyond the observed rainfall maximum the agreement between the observed rainfall distribution and the orographic rainfall distribution computed from the present model is better than that computed from the approximate model. At the crest ($x = 5$ km.) of the mountain, the orographic rainfall computed from the present model is 1.4 mm./hr. compared to the observed intensity of 2.8 mm./hr. The corresponding value from the approximate model is nil. The computed orographic rainfall on the lee side from the present model extends to $x = 45$ km. (i.e., to Poona) with a secondary maximum of 0.6 mm./hr. at $x = 24$ km., although the lee-side computed rainfall is small compared to the observed rainfall.

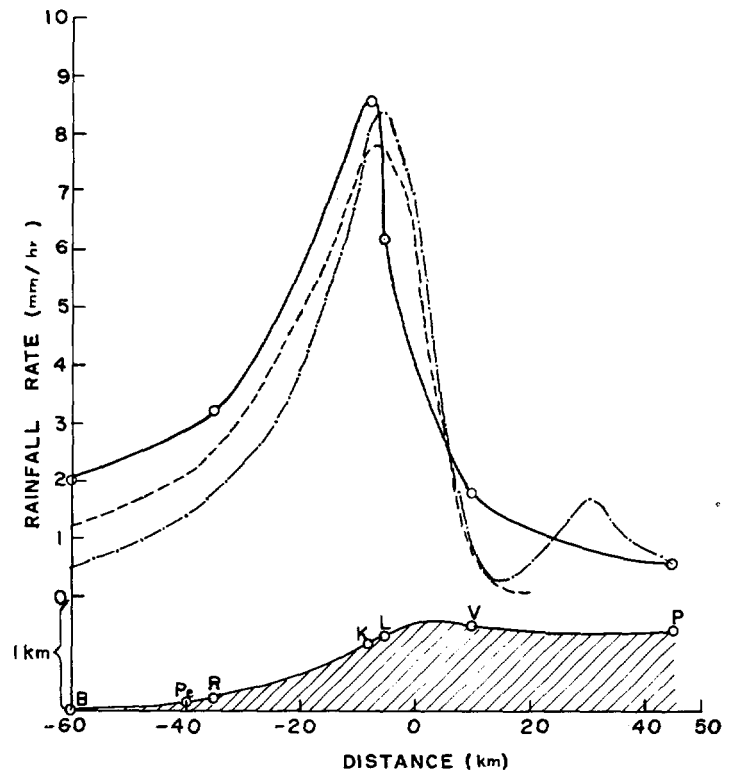


FIGURE 4.—Rainfall distribution for June 25, 1961 (Case II). See legend for figure 3.

CASE IV—JULY 11-12, 1965

Vertical velocity from the coast to $x = -20$ km., is more in the approximate model than that in the present model. The maximum vertical velocity from the approximate model is 33 cm. sec.^{-1} at $x = -10$ km. and the corresponding value from the present model is 48 cm. sec.^{-1} . In the approximate model, vertical velocity is negative at all levels beyond $x = 0$ km. But in the present model, beyond $x = 2$ km. velocity is positive above 3 km. as a result of the lee wave of length 31 km. and this continues to $x = 17$ km.

The rainfall distributions, observed and computed, are given in figure 6. The approximate model appears to show that rainfall from the coast to the position of the rainfall maximum is entirely due to orography. But this is not so, when we see the orographic distribution computed from the present modified model. At the coast, the computed orographic precipitation from the present model is only 0.5 mm./hr. compared to the observed intensity of 2.2 mm./hr. The maximum orographic rainfall computed from the present model is 92 percent of the observed maximum rainfall, the corresponding figure from the approximate model being 90 percent. There is close agreement between the positions of the observed and computed maximum rainfalls. Unlike the previous cases, the agreement between the observed rainfall distribution and the computed rainfall distribution beyond the positions of rainfall maxima is not so good. However, the present

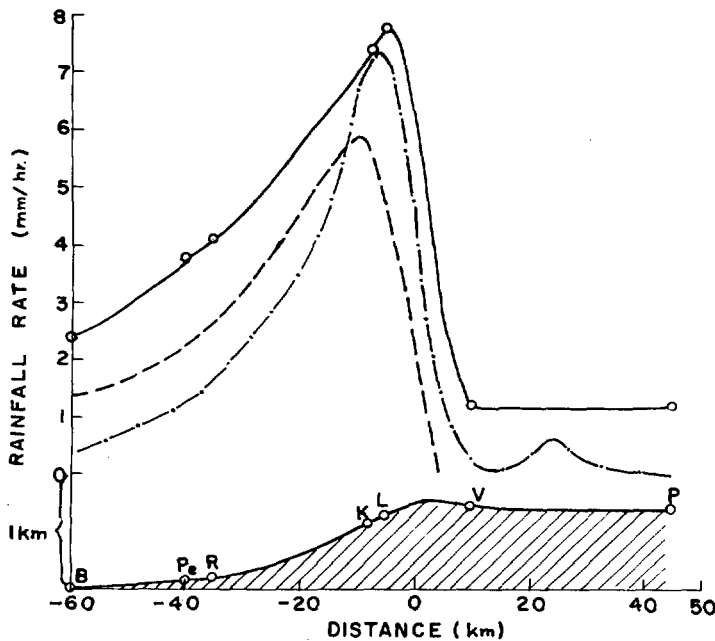


FIGURE 5.—Rainfall distribution for July 6-9, 1963 (Case III). See legend for figure 3.

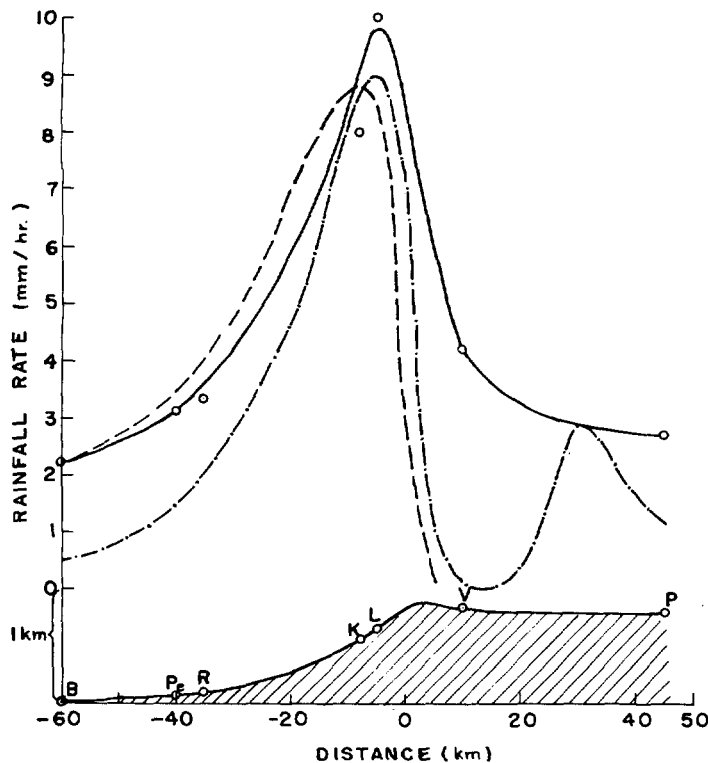


FIGURE 6.—Rainfall distribution for July 11-12, 1958 (Case IV). See legend for figure 3.

model definitely explains better the rainfall distribution than does the approximate model. At the crest of the mountain, the observed rainfall is about 6 mm./hr. The computed orographic rainfall there is 1.4 mm./hr. for the present model and nil for the approximate model. For the present model the computed orographic rainfall on the lee side extends beyond $x=45$ km. (i.e., beyond Poona) with a secondary maximum of 2.9 mm./hr. at $x=30$ km.

CASE V—JULY 21, 1959

Vertical velocity from the coast to $x=-20$ km. as given by the approximate model is more than that given by the present model. For example at $x=-50$ km., the maximum vertical velocity for the approximate model is 7.0 cm. sec.⁻¹, but that in the present model is 2.5 cm. sec.⁻¹. The velocity is maximum at $x=-10$ km. in both the models. These values are 32.5 cm. sec.⁻¹ and 38.5 cm. sec.⁻¹ in the approximate and the present model, respectively. Beyond $x=1$ km. vertical velocity is negative at all levels in the approximate model. But in the present modified model, velocity is positive at low levels and negative at high levels to $x=3$ km., beyond which velocity is negative at low levels and positive at high levels, i.e., above 4.5 km. or so. This corresponds to the wave of length 26 km. This continues to $x=15$ km.

The rainfall distributions, observed as well as computed from the two models, are given in figure 7. The computed orographic rainfall from the approximate model appears to show that the entire rainfall on the windward side in this case is due to orography. But the present model shows that it is not so. The observed rainfall at the coast is 1.8 mm./hr. and the orographic rainfall computed from the approximate model is 1.7 mm./hr. But the corresponding value from the present model is 0.3 mm./hr. only. The orographic maximum rainfall from the present model is 7.8 mm./hr. and it is 93 percent of the observed maximum rainfall. The orographic maximum, computed from the approximate model, on the other hand, slightly exceeds the observed maximum. The positions of the rainfall maxima differ at most by 2 km. However, in this case the position and magnitude of the observed maximum rainfall is a bit subjective as the rainfall of Lonavla (which is very near Khandala) is not available. Beyond the rainfall maxima, the orographic rainfall computed from the present model explains better the actual rainfall than that computed from the approximate model. At the crest of the mountain the observed rainfall is 3.0 mm./hr. and the orographic rainfall computed from the present model is 2.8 mm./hr. The computed orographic rainfall from the present model extends beyond $x=45$ km. (i.e., Poona) on the lee side with a secondary maximum of 1.0 mm./hr. at $x=26$ km.

6. CONCLUSION

We can draw the following conclusions from the present investigation:

(i) The orographic rainfall, computed from the present modified model as well as from the approximate model, increases from coast to inland along the slope and reaches a maximum before the crest of the mountain is reached, after which it falls off sharply. This is well in agreement with the observed rainfall distribution in all the cases studied here. The normal rainfall during the southwest monsoon also is seen to have a similar distribution.

(ii) The positions of the maximum observed rainfall and the computed maximum orographic rainfall are in excellent agreement. They generally occur at 10–12 km. before the crest of the mountain.

(iii) In [6], we saw that the approximate model accounts for, in general, 60 percent of the coastal rainfall. But the present modified model shows that the contribution of orography to coastal rainfall is very meager, viz, hardly 20 percent. This suggests that most of the coastal rainfall is due to synoptic-scale convergence and instability. Beyond about 30 km. from the coast the effect of orography becomes dominant.

(iv) The modified model accounts in all the five cases for 93 to 98 percent of the observed maximum rainfall. The peak in the rainfall distribution is, therefore, purely an orographic effect. This was also the finding in [6] for the approximate model, but is more prominent in the present model.

(v) In [6] we concluded from the approximate model that the rainfall on the lee side is not due to orography. But the present model does suggest that rainfall due to

orography may extend to 40 km. from the crest of the mountain and thus explains a part of the lee-side rainfall. Also the computed orographic distribution has a secondary maximum on the lee side at about a distance of 25 km. from the crest, with a region of no or negligible rainfall just before it. The lee-side precipitation is caused by ascending motion associated with waves of length 20–30 km.

We, however, could not verify the secondary maximum in computed rainfall, as we do not have any rain-reporting stations between the two lee-side stations Vadgaon and Poona which are at a distance of 35 km. from each other.

We should also be cautious about the computed lee-side rainfall, as on this side the atmosphere may not be saturated as envisaged in our model.

(vi) The ascending motion in the present model on the windward side and on the lee side suggests that rainfall on the windward side originates at low levels below 5 km. and that on the lee side has a high-level origin above 5 km. This ties in well with the radar observations (Pisharoty [5] and Mani et al. [3]). These observations show that the precipitation on the west of the Ghats and up to the crest, comes from clouds the tops of which are below the freezing level, and only the condensation-coalescence process is involved in the initiation of rain in this region. Over the rain-shadow region on the lee, most of the rain is from above the freezing level as is evidenced by the "bright bands" of rain echoes and is initiated by the Bergeron process through ice nucleation.

However, although we note that the modified model suggested here explains the observed rainfall distribution quite satisfactorily, it is not free from limitations. And the discrepancies between the observed rainfall and the rainfall computed from the model can be attributed to the following reasons: (a) We have taken a simplified smoothed profile for the terrain which in reality is not so. (b) Our assumption of steady streamline flow in a statically neutral atmosphere may not be fully representative of the real atmosphere which is sometimes to some extent unstable as compared to the pseudo-adiabatic lapse rate. (c) Rainfall may not be entirely due to orography, at least not near the coast. Rainfall may occur as a result of lifting of saturated air from other causes as well, viz, horizontal convergence in the synoptic scale and instability. It is quite likely that rainfall in mountain areas results from the three causes operating together.

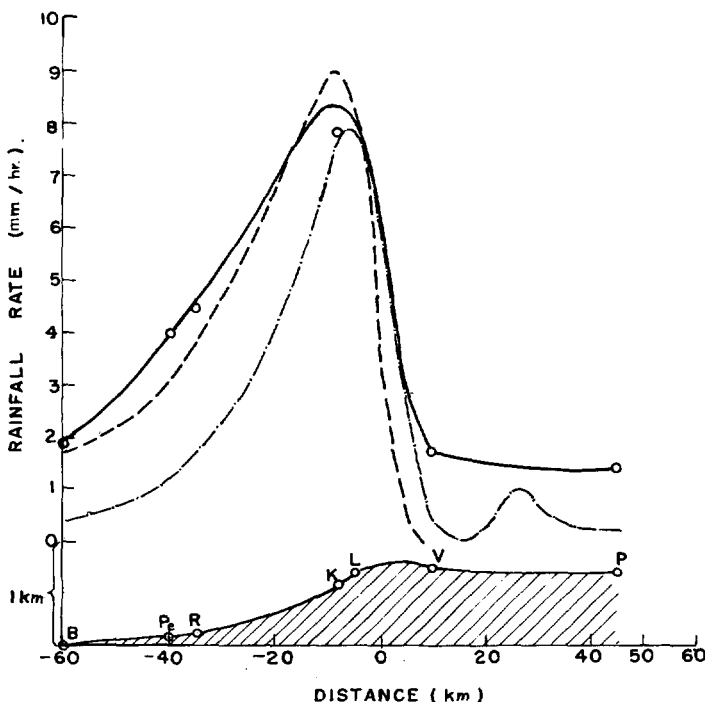


FIGURE 7.—Rainfall distribution for July 21, 1958 (Case V). See legend for figure 3.

ACKNOWLEDGMENTS

I am thankful to the Director of the Institute of Tropical Meteorology, Poona, for giving me facilities to carry out the investigation; to the Tata Institute of Fundamental Research, Bombay, for allowing me to carry out the numerical programs with their electronic computer CDC 3600; and to Mr. N. S. Kulkarni and Mr. M. B. Pant for help in some computations.

REFERENCES

1. G. A. Corby and J. S. Sawyer, "The Airflow over a Ridge: The Effects of the Upper Boundary and High Level Conditions," *Quarterly Journal of the Royal Meteorological Society*, vol. 84, No. 359, Jan. 1958, pp. 25-37.
2. T. N. Krishnamurti, "The Finite Amplitude Mountain Wave Problem With Entropy as a Vertical Coordinate," *Monthly Weather Review*, vol. 92, No. 4, Apr. 1964, pp. 147-160.
3. A. Mani, B. B. Huddar, and G. P. Srivastava, "Studies of 'Melting Band' in Radar Precipitation Echoes at Poona and Bombay During the Monsoon," *Indian Journal of Meteorology and Geophysics*, vol. 13, Special No., Mar. 1962, pp. 127-136.
4. E. Palm and A. Foldvik, "Contribution to the Theory of Two Dimensional Mountain Waves," *Geofysiske Publikasjoner*, vol. 21, No. 6, Mar. 1960, 30 pp.
5. P. R. Pisharoty, "Dynamics of the Monsoon Rain at Poona," *Indian Journal of Meteorology and Geophysics*, vol. 13, Special No., Mar. 1962, pp. 65-72.
6. R. P. Sarker, "A Dynamical Model of Orographic Rainfall," *Monthly Weather Review*, vol. 94, No. 9, Sept. 1966, pp. 555-572.
7. R. P. Sarker, "A Theoretical Study of Mountain Waves on Western Ghats," *Indian Journal of Meteorology and Geophysics*, vol. 16, No. 4, 1965, pp. 565-584.
8. J. S. Sawyer, "Numerical Calculation of the Displacements of a Stratified Airstream Crossing a Ridge of Small Height," *Quarterly Journal of the Royal Meteorological Society*, vol. 86, No. 369, July 1960, pp. 326-345.

[Received May 2, 1967]